Inorganic Chemistry

Article

pubs.acs.org/IC

Solvent-Induced Structural Dynamics in Noninterpenetrating Porous Coordination Polymeric Networks

Raghavender Medishetty,[†] Daram Jung,[‡] Xiaokai Song,[§] Dongwook Kim,[§] Shim Sung Lee,*[,‡] Myoung Soo Lah,*[,§] and Jagadese J. Vittal*[,†,‡]

[†]Department of Chemistry, National University of Singapore, 3 Science Drive 3, 117543, Singapore

[‡]Department of Chemistry and Research Institute of Natural Science, Gyeongsang National University, Jinju 660-701, Korea

[§]Interdisciplinary School of Green Energy, Ulsan National Institute of Science and Technology, Ulsan 689-798, Korea

Supporting Information

ABSTRACT: Three novel soft porous coordination polymer (PCP) or metal−organic framework (MOF) compounds have been synthesized with a new rigid ligand *N*-(4-pyridyl)-1,4,5,8-naphthalenetetracarboxymonoimide (PNMI) by partial hydrolysis of *N,N′*-di-(4-pyridyl)-1,4,5,8-naphthalenete-tracarboxydiimide (DPNI) during solvothermal reactions with Zn(II), Cd(II), and Mn(II) salts, and they are [Zn(PNMI)]·2DMA (**1**·2DMA, **1a**), [Cd-(PNMI)]·0.5DMA·5H_2O (**2**·0.5DMA·5H_2O), and [Mn-(PNMI)]·0.75DMF (**3**·0.75DMF). The structure of **1** is based on paddle-wheel secondary building unit (SBU) with a 3,6-connected **rtl** net topology, whereas **2** and **3** are isotypical but the $M(O_2C-C)_2$ fragments aggregate in one-dimension and the overall connectivity is the same **rtl** net topology. All these three MOFs have one-dimensional rhombic channels filled with guest molecules. The guest molecules in **1a** can be exchanged with EtOH in a single-crystal to single-crystal (SCSC) manner to **1**·1.25EtOH·0.375H_2O (**1b**). Further, the guest molecules in **1b** can be replaced with ethylene glycol, triethylene glycol and allyl alcohol without destroying its single crystal nature. These guest exchanges are accompanied by reduction in volume of the unit cell up to 16%, as well as the void volume up to 33.1%. Similarly, triethylene glycol (TEGly) selectively exchanges EtOH in a mixture of the above solvents, which might be the result of correct fit of the hydrogen-bonded TEGly dimer in the channel of **1**. While activated **1** and **3** exhibit no uptake of N_2 and H_2 at 1 bar and 77 K and very low uptake of CO_2 gas at 1 bar and 196 K, activated **2** shows selective CO_2 uptake, 278 $cm^2 \cdot g^{-1}$, over N_2 and H_2 at 1 bar and 196 K, which corresponds to 5.87 molecules of CO_2 per formula unit of **2**.

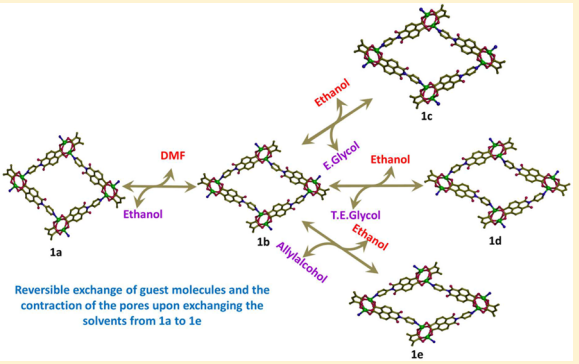

INTRODUCTION

In the past two decades, porous coordination polymers (PCPs) or metal−organic frameworks (MOFs) attained a tremendous amount of growth not only because of their connectivity, topologies, and structural patterns[1] but also their diverse potential applications in gas storage, separation, catalysis, lithium ion batteries, and sensors.[2] Among these, flexible or soft porous networks which is also called the third generation of PCPs have generated interests because of their structural dynamics compared to the rigid MOFs.[3] This dynamic nature seems to be advantageous for the development of new materials for separation of gas mixtures.[3a,4] Numerous flexible MOFs have been reported, which are mainly derived from flexible ligands[5] but limited literature is also available on flexible MOFs containing flexible SBUs.[3f] Recently, Kitagawa et al. discussed flexible nature of Zn(II) paddle-wheel secondary building unit (SBU) upon evacuating the compound and transforming into tetrahedral coordination geometry through an intermediate state.[5] Meanwhile, DFT calculations also supported the flexibility in Zn(II) paddle-wheel SBU.[6] However, monitoring this flexible nature of soft SBU in the dynamic process requires single crystals after the removal or exchange of guest molecules. Though there are few reports available in the guest exchange process,[7] it is still very hard to study the structural dynamics through exchanging the guest molecules via single-crystal to single-crystal (SCSC) manner.[8] The exchange of guest molecules can make and break different supramolecular interactions with the main structure together with the change in size and shape of the space occupied by different guest molecules in the exchange process and these create strain to make the crystal break.

The emission of CO_2 is one of the major environmental issues in global warming. An easier solution to control the CO_2 in the atmosphere is to capture the gas using nonchemical and eco-friendly processes. A number of MOFs have been found to be suitable for this purpose by physisorption due to large surface area, pore volume and ease in the cycling process.[2c]

Received: October 25, 2012
Published: March 1, 2013

   dx.doi.org/10.1021/ic302334x | *Inorg. Chem.* 2013, 52, 2951−2957

However, designing these materials is one of the challenging processes because of the preparation of these compounds with specific functional groups exposed toward the pores, which can interact with the gas molecules.[9] This current work presents synthesis of three porous MOFs, where the pore is mainly exposed with highly polar imide oxygen atoms suitable to interact with the quadrupolar gas molecules such as CO_2.[10] The ligand *N*-(4-pyridyl)-1,4,5,8-naphthalenetetracarboxymonoimide (PNMI) used in these MOFs were obtained inadvertently by the partial hydrolysis of *N,N′*-di-(4-pyridyl)-1,4,5,8-naphthalenetetra-carboxydiimide (DPNI) in the solvothermal reactions. The solid state structures of all the three MOFs possess rhomboidal channels. The soft and flexible nature of the Zn(II) MOF was established through various guest exchange reactions in an SCSC manner. The Cd(II) MOF shows selective CO_2 uptake 278 $cm^3 \cdot g^{-1}$ at 196 K over H_2, N_2, Ar, and CH_4.

EXPERIMENTAL SECTION

Materials and General Methods. Commercially available reagent grade chemicals were used as received without any further purification unless mentioned. IR spectra were recorded on a FTS165 Bio-Rad FTIR spectrometer by using KBr pellets in the range of 4000−400 cm^{-1}. Elemental analyses (C, H, and N) were carried out using Elementar Vario Micro Cube instrument at the Elemental Analysis Lab, CMMAC, Department of Chemistry, National University of Singapore. Thermogravimetric analysis (TGA) was performed under N_2 atmosphere with the heating rate of 5 °C min^{-1} on a SDT 2960 Thermal analyzer. NMR spectra were recorded on 300 MHz FT-NMR spectrometer in d_6-DMSO solvent. The powder X-ray diffraction (PXRD) patterns were recorded on a Siemens D500 diffractometer with graphite monochromated Cu Kα radiation (λ = 1.54056 Å) at 298 K. DPNI ligand has been synthesized according to a reported method.[11]

Synthesis of [Zn(PNMI)]·2DMA (1·2DMA, 1a). A mixture of $Zn(NO_3)_2 \cdot 6H_2O$ (3.7 mg, 0.0125 mmol) and DPNI (5 mg, 0.0125 mmol) were added to DMA (2 mL), pyridine (1 mL), and water (0.5 mL) in 20 mL glass vial and the reaction solution was sonicated until it gave a clear solution and then placed it in a programmable oven and heated it at 120 °C for 48 h, followed by cooling to room temperature at the rate of 5 °C·h^{-1}. Light yellow needle-shaped crystals were obtained. These crystals were washed with DMA and water and dried under vacuum. Yield: 38% (based on DPNI). Calcd for $C_{19}H_8N_2O_6Zn \cdot 2C_4H_9NO$ (FW = 599.91): C, 54.06; H, 4.37; N, 9.34. Found: C, 54.28, H, 4.43, N, 9.27. Selected IR (KBr): ν (cm^{-1}) = 3404 (s), 1707 (m), 1661 (s), 1570 (s), 1442 (s), 1381 (s), 1352 (s), 1242 (s), 1195 (m), 863 (m), 816 (m), 775 (s), (m). TG weight loss observed: 29.7%; calculated 29.1% (for the loss of 2 DMA molecules).

Synthesis of [Zn(PNMI)]·1.25EtOH·0.375H_2O (1b). The single crystals of compound **1a** were soaked in ethanol for two days. The DMA molecules in the solvent channels have been exchanged with ethanol and water retaining the single crystallinity suitable for X-ray data collection. TG weight loss observed: 17.7%. Calculated: 18.1% (for the loss of 1.25 EtOH and 0.375 H_2O molecules).

Synthesis of [Cd(PNMI)]·0.5DMA·5H_2O (2·0.5DMA·5H_2O). A mixture of $Cd(NO_3)_2 \cdot 4H_2O$ (7.7 mg, 0.025 mmol) and DPNI (10 mg, 0.025 mmol) were added to 1.5 mL of DMA, 1 mL of water, and 1 mL of methanol in 20 mL scintillation vial and heated at 90 °C for 48 h followed by cooling to room temperature at the rate of 4 °C·h^{-1}, resulted in light yellow block crystals which were filtered and washed with fresh DMA and methanol and dried at room temperature. Yield: 80% (based on DPNI). Elemental analysis (%) Calcd for $C_{19}H_8N_2O_6Cd$ (472.69) (desolvated sample): C, 48.28; H, 1.71; N, 5.93. Found: C, 48.53; H, 2.22; N, 5.97. Selected IR (KBr): ν (cm^{-1}) = 3433 (m), 1710 (m), 1663 (s), 1588 (s), 1438 (m), 1380 (s), 1241 (m), 775 (s), 659 (m), 439 (m). TG weight loss observed: 24.0%; calculated 22.0% (for the loss of half DMA and five water molecules).

Synthesis of [Mn(PNMI)]·0.75DMF (3·0.75DMF). A mixture of $Mn(ClO_4)_2 \cdot 4H_2O$ (4.25 mg, 0.025 mmol) and DPNI (5 mg, 0.0125 mmol) in 2 mL of DMF, 1 mL water and 100 μL of 1 M $HClO_4$ kept in 20 mL scintillation vial and heated at 80 °C for 48 h followed by cooling to room temperature at the rate of 4 °C·h^{-1} resulted in light yellow crystals of **2**, which were washed with fresh DMF and water and dried at room temperature. Yield: 62% (based on DPNI). Calcd for $C_{19}H_8N_2O_6Mn$ (415.21) (desolvated sample): C, 54.96; H, 1.94; N, 6.75 Found: C, 54.96; H, 2.18; N, 6.71. Selected IR (KBr): ν (cm^{-1}) = 3404 (s), 1707 (m), 1661 (s), 1570 (s), 1442 (s), 1381 (s), 1352 (s), 1242 (s), 1195 (m), 863 (m), 816 (m), 775 (s).

Caution! *Perchlorate salts are potentially explosives. Although we did not have any unpleasant experience probably due to the usage of a very small amount, care should be taken to avoid any untoward experience.*

X-ray Crystallography. Structural data for all these compounds were collected at 100(2) K on Bruker APEX diffractometer attached with a CCD detector and graphite-monochromated Mo Kα (λ = 0.71073 Å) radiation through a sealed tube (2.4 kW). An empirical absorption correction was applied to the data by using the SADABS[12] program and the crystallographic package SHELXTL[13] was used for all calculations.

Crystal Data for 1a at 173(2) K. $C_{27}H_{26}N_4O_8Zn$, M = 599.89, monoclinic, $P2_1/c$; a = 5.6364(6) Å, b = 25.301(3) Å, c = 18.8863(2) Å, β = 95.470(2)°, V = 2681.0(5) $Å^3$, Z = 4, ρ_{calcd} = 1.486 $g.cm^{-3}$, μ = 0.974 mm^{-1}, GOF = 1.036, final R1 = 0.0607, wR2 = 0.1578 [for 3974 data $I > 2\sigma(I)$].

Crystal Data for 1b at 173(2) K. $C_{43}H_{32.50}N_4O_{15.25}Zn_2$, M = 979.97, monoclinic, $P2_1/c$; a = 5.5871(2) Å, b = 25.9462(9) Å, c = 17.4983(7) Å, β = 96.031(2)°, V = 2522.6(2) $Å^3$, Z = 2, ρ_{calcd} = 1.290 $g \cdot cm^{-3}$, μ = 1.016 mm^{-1}, GOF = 1.082, final R1 = 0.0550, wR2 = 0.1746 [for 4761 data $I > 2\sigma(I)$].

Crystal Data for1c at 173(2) K. $C_{44}H_{43}N_4O_{22.50}Zn_2$, M = 1118.56, monoclinic, $P2_1/c$; a = 5.6137(2) Å, b = 26.3769(9) Å, c = 17.1499(6) Å, β = 96.820(2)°, V = 2521.5(2) $Å^3$, Z = 2, ρ_{calc} = 1.473 $g.cm^{-3}$, μ = 1.036 mm^{-1}, GOF = 1.090, final R1 = 0.0530, wR2 = 0.1584 [for 3961 data $I > 2\sigma(I)$].

Crystal Data for 1d at 173(2) K. $C_{50}H_{42}N_4O_{20}Zn_2$, M = 1149.62, monoclinic, $P2_1/c$; a = 5.5797(4) Å, b = 25.9231(2) Å, c = 16.7931(1) Å, β = 98.575(4)°, V = 2401.9(3) $Å^3$, Z = 2, ρ_{calcd} = 1.590 $g \cdot cm^{-3}$, μ = 1.087 mm^{-1}, GOF = 1.095, final R1 = 0.0501, wR2 = 0.1159 [for 3790 data $I > 2\sigma(I)$].

Crystal Data for 1e at 100(2) K. $C_{47}H_{38}N_4O_{17}Zn_2$, M = 1061.55, monoclinic, $P2_1/n$; a = 5.6415(14) Å, b = 27.633(7) Å, c = 14.847(4) Å, β = 100.149(4)°, V = 2278.3(10) $Å^3$, Z = 2, ρ_{calcd} = 1.547 $g \cdot cm^{-3}$, μ = 1.134 mm^{-1}, GOF = 1.076, final R1 = 0.0656, wR2 = 0.1677 [for 3382 data $I > 2\sigma(I)$].

Crystal Data for 2 at 100(2) K. $C_{42}H_{45}Cd_2N_5O_{23}$, M = 1212.63, monoclinic, $P2_1/n$; a = 4.9738(5) Å, b = 24.836(3) Å, c = 20.663(2) Å, β = 95.903(3)°, V = 2538.9(4) $Å^3$, Z = 2, ρ_{calcd} = 1.586 $g \cdot cm^{-3}$, μ = 0.923 mm^{-1}, GOF = 1.068, final R1 = 0.0774, wR2 = 0.1362 [for 4615 data $I > 2\sigma(I)$].

Crystal Data for 3 at 173(2) K. $C_{21.25}H_{13.25}MnN_{2.75}O_{6.75}$, M = 470.04, monoclinic, $P2_1/n$; a = 5.0169(3) Å, b = 24.9851(17) Å, c = 20.6949(17) Å, β = 95.721(4)°, V = 2581.1(3) $Å^3$, Z = 4, D_{calcd} = 1.210 $g \cdot cm^{-3}$, μ = 0.550 mm^{-1}, GOF = 1.129, final R1 = 0.1058, wR2 = 0.3005 [for 4246 data $I > 2\sigma(I)$].

Sorption Measurements. All gas sorption isotherms were measured using a BELSORP-max (BEL Japan, Inc.) with a standard volumetric technique using N_2 (with purity of 99.999%), Ar (99.9999%), H_2 (99.9999%), CO_2 (99.999%), and CH_4 (99.95%) as adsorbates. Compounds **1** and **3** were activated at RT for around a day under vacuum, and compound **2** was activated at 150 °C for 14 h under vacuum and studied the gas sorption studies. The adsorption data in the pressure range lower than ~0.1 bar P/P0 were fitted to the Brunauer−Emmett−Teller (BET) equation to determine the BET specific surface area. The entire set of adsorption data was used to obtain the Langmuir specific surface area.

dx.doi.org/10.1021/ic302334x | *Inorg. Chem.* 2013, 52, 2951−2957

RESULTS AND DISCUSSION

In all the three syntheses, solvothermal reactions between the metal salts and DPNI in a mixture of DMF and water resulted in single crystals containing a partially hydrolyzed product of DPNI. In this new ligand, *N*-(4-pyridyl)-1,4,5,8-naphathalene-tetracarboxy-monoimide (PNMI), one of the imide groups of DPNI hydrolyzed under the reaction conditions employed as shown in Scheme 1.

Scheme 1. PNMI as a Partial Hydrolysis Product of DPNI Ligand

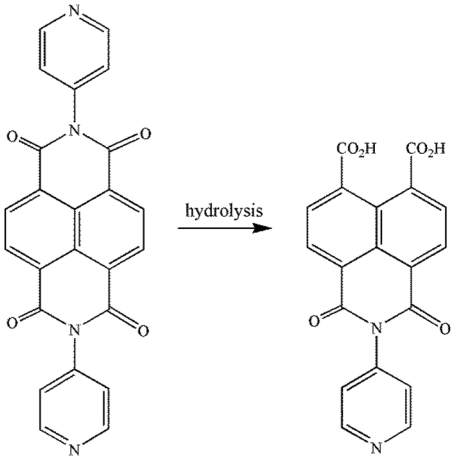

It appears that the extent of hydrolysis depends on the nature of metal ion used, as indicated by the yield that varies in the range 38−80%. The formation of uniform products in these reactions was confirmed by a comparison of powder X-ray diffraction pattern with that generated from the single crystal data and elemental analysis. The DPNI has been used in a number of solvothermal syntheses of about 10 different coordination polymers;[10a,11,14] to our surprise such hydrolysis has not been reported so far. Here we describe the crystal structures of three structurally similar coordination polymers, of which two are isotypical, formed by this interesting and unique ligand, PNMI.

Crystal Structures. The asymmetric unit of [Zn(PNMI)]·2DMA (**1**·2DMA, **1a**) consists of a Zn(II), one PNMI ligand and two DMA lattice solvents. The structure consists of the well-known paddle-wheel SBU in which the two Zn(II) have a distorted square pyramidal geometry. Each paddle-wheel SBU is coordinated by carboxylates groups from four different PNMI ligands and the two apical positions are occupied by pyridyl-N atoms from two different PNMI ligands forming a 3D porous structure as shown in Figure 1a. On the other hand, the two carboxylates from the same PNMI ligand is bonded to two adjacent Zn(II) pairs in the paddle wheels. Crystallographic inversion center is present in the middle of these paddle wheel SBU units. This connectivity generates rhombic channels along the *a*-axis as shown in Figure 1b. The connectivity can be simplified as a 3,6-connected binodal network of an **rtl** net topology with point symbol $(4{\cdot}6^2)_2(4^2{\cdot}6^{10}{\cdot}8^3)$ (see Supporting Information Figure S1) by considering PNMI as a three connected node and the paddle-wheel SBU as a six connected node.[15]

The diagonal distances between the centers of paddle-wheels in the rhombic channels are 25.301(3) and 18.886(2) Å (*b* and *c* axes of the unit cell). The channels are filled with DMA molecules. PLATON[16] shows the total potential solvent area volume is 1290.5 Å^3 (i.e., 48.1% per unit cell volume, 2681.0 Å^3) after removing these two DMA molecules.

Guest Replacement by Single-Crystal to Single-Crystal Process. These DMA molecules in **1a** can easily be exchanged with ethanol without destroying its single crystal nature. The solvents in these single crystals of **1**·1.25EtOH·0.375H_2O (**1b**) can be further replaced by ethylene glycol (EG), triethylene glycol (TEGly), and allyl alcohol (AllylOH) by soaking **1b** in the respective guest liquids to give **1**·0.5EG·0.75H_2O (**1c**), **1**·TEGly (**1d**), and **1**·1.25AllylOH·1H_2O (**1e**), respectively. The crystal structures of all these compounds have been determined from the single-crystal X-ray diffraction experiments. The cell data and relevant information of the guest exchanged crystals are shown in Table 1.

For instance, when **1a** was exchanged with ethanol, there is a decrease in the cell volume (2681−2522.6 Å^3) in **1b** as well as reduction in the porosity (48.1−44.8%). The reduction in cell volume is maximal for **1e** and as a result the pore volume is also drastically reduced to 37.9%. This shows the breathing and dynamic nature of this framework which can also be understood by comparing the diagonal distances of the rhombic

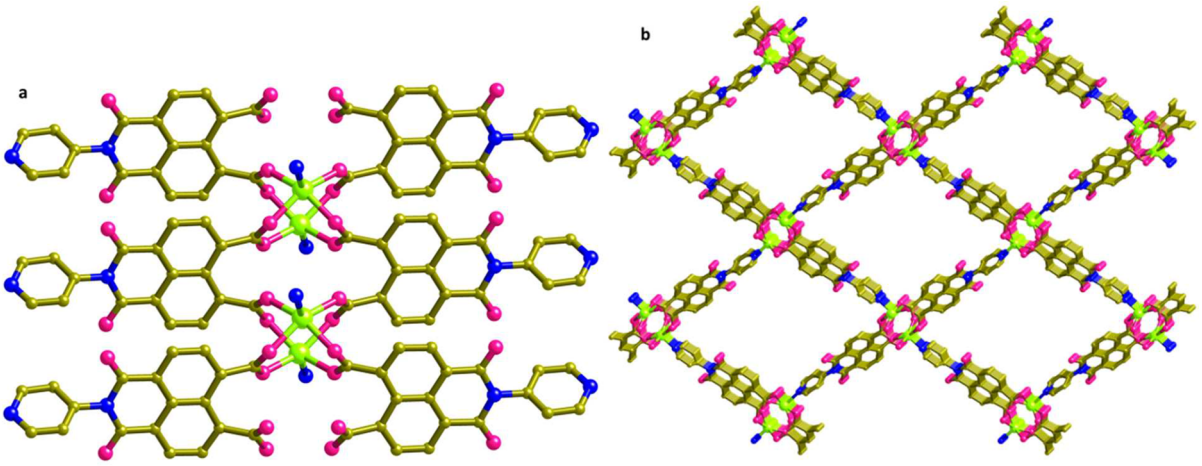

Figure 1. (a) Coordination geometry and connectivity in **1a**. (b) A portion of the 3D structure of **1a** viewed along *a*-axis. The guest molecules and the hydrogen atoms have been omitted for clarity.

dx.doi.org/10.1021/ic302334x | *Inorg. Chem.* 2013, 52, 2951−2957

Table 1. Cell Data for 1a−e, 2, and 3

crystal	a (Å)	b (Å)	c (Å)	β (deg)	V (Å^3)	void [Å^3 (%)]	∠PNMI−Zn SBU−PNMI (deg)
1a	5.6364(6)	25.301(3)	18.886(2)	95.470(2)	2681.0(5)	1290.5 (48.1)	105.6
1b	5.5871(2)	25.9462(9)	17.4983(7)	96.031(2)	2522.6(2)	1130.7 (44.8)	111.1
1c	5.6137(2)	26.3769(9)	17.1499(6)	96.820(2)	2521.5(2)	1122.7 (44.5)	113.2
1d	5.5797(4)	25.923(2)	16.793(1)	98.575(4)	2401.9(3)	1003.4 (41.8)	113.8
1e	5.642(1)	27.633(7)	14.847(4)	100.149(4)	2278.3(10)	863.0 (37.9)	123.5
2·0.5DMA·5H_2O	4.9738(5)	24.836(3)	20.663(2)	95.903(3)	2538.9(4)	1138.8 (44.9)	96.5
3·0.75DMF	5.0169(3)	24.985(2)	20.695(2)	95.721(4)	2581.1(3)	1083.7 (42.0)	110.0

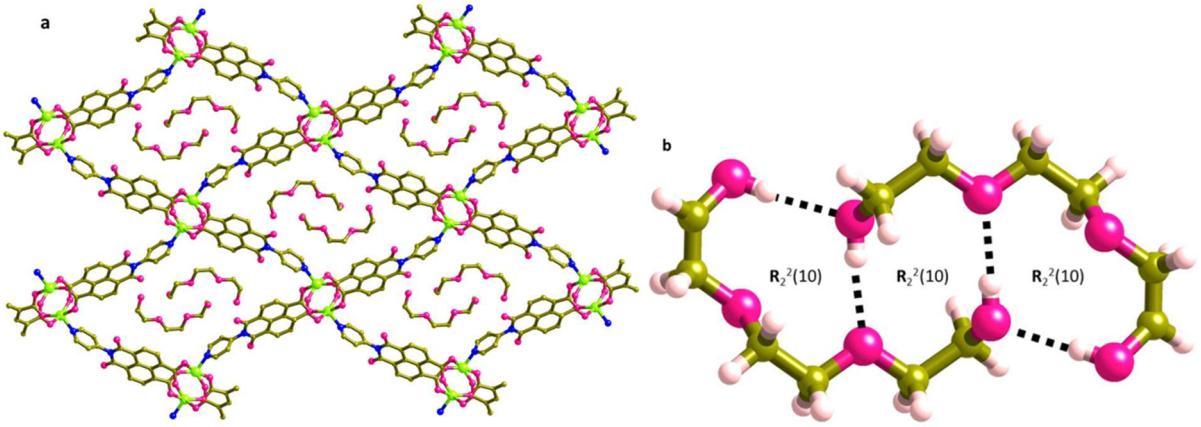

Figure 2. (a) Portion of the structure showing the arrangement of the guest triethyleneglycol in **1d**. (b) Hydrogen-bonded triethyleneglycol dimer in **1d**.

channels in these crystals in Table 1. The length of the *b*-axis in the unit cell increased from 25.301(3) Å in **1a** to 27.633(7) Å in **1e**, while the length of the *c*-axis has contracted from 18.886(2) Å in **1a** to 14.847(4) Å in **1e**. This is reflected in the distortion of the rhomboidal framework. As we go down from **1a** to **1e** in the Table 1, the angle subtended by the equatorial and axial PNMI ligands with respect to the paddle-wheel unit has increased from 105.65° to 123.50° (see Supporting Information Figure S2). Such shape responsive fitting of guest molecules have been observed before.[17]

In the structures obtained by exchanged guest molecules **1b**, **1c**, and **1e**, either a mixture of solvents have been incorporated or the guest molecules have been partially occupied or disordered in the channels. But in the case of **1d** where the channel is occupied by the TEGly as shown in Figure 2a, a perfectly ordered hydrogen-bonded dimer has formed through complementary H-bonding (see Figure 2b). This guest dimer is forming three ten-membered hydrogen-bonded rings within the channel of **1d**. Although this TEGly ligand is a popular multidentate ligand for lanthanide metal ions, there is only one crystal structure reported to have crystallized TEGly as a guest molecule with no aggregation.[18] It appears that the channels in **1** provided a tight fit for this hydrogen-bonded TEGly dimer, which has never been observed before. Similarly, all these guest molecules in **1c**, **1d**, and **1e** can be exchanged with ethanol by soaking these crystals in ethanol. Further when the single crystals of **1b** was dropped into the 1:1:1 solution of EG, TEGly, and allylalcohol, the ethanol molecules in **1b** are selectively replaced exclusively by TEGly as monitored by ^{1}H NMR spectroscopy. This could be attributed to the correct fit of the hydrogen-bonded TEGly dimer in the channels of **1** compared to other guest molecules (Supporting Information Figure S3). Further, all the single crystals of **1a−1e** do not survive without the guest molecules. This could be due to the strain created by severe distortion of the channel shape on guest removal. However, the PXRD patterns confirmed that they still retain the same crystal structure (Supporting Information Figure S4).

From the dynamic behavior of this compound one might anticipate to generate little or no porosity due to distortion in the channels, however some specific guest molecules can reopen these channels expected to give hysteretic adsorption.[3f,h] On the other hand, the pores have been found closed in many interpenetrated structures due to the movements of the different frames closer to each other to fill in the empty space.[19]

A closer look at the structure reveals that the metal(II) atoms have been away from the plane of the pyridyl ring to which it is bonded. This distortional parameters namely, the angle of deviation from planarity and the distance from the plane of the pyridyl ring bonded, have been collected in Supporting Information Table S1. For **1a−1e**, these deviations are pronounced and are in the range 14.2−26.1° and 0.51−0.94 Å. But there is no trend observed that can be correlated to any of the parameters listed in Table 1. Maximal distortion occurs in **1d** (26.1° and 0.94 Å) where highly ordered hydrogen-bonded TEGly dimers have been occupied the channel. It appears that the overall structure is stabilized by these hydrogen-bonded TEGly dimers at the cost of this distortion. Such a highly distorted MOF structure stabilized by weak hydrogen bonding interactions seems to be very unusual. On the contrary, these distortional parameters are smaller for **2** and **3** as compared to **1** probably providing robustness by the more rigid octahedral environment (see Figure 4a).

Another interesting observation of the structural data for **1a−1e** is their simulated XRPD patterns. These structures can be considered as isomorphous and isostructural in nature with different guest molecules occupying the channels, despite large variation in the *a* and *b* axes. However, from the simulated

dx.doi.org/10.1021/ic302334x | *Inorg. Chem.* 2013, 52, 2951−2957

XRPD patterns of **1a**−**1e** shown in Figure 3, it is difficult to predict they are indeed isomorphous and isostructural. Hence if

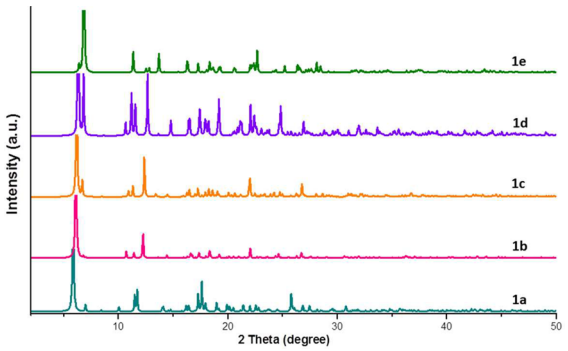

Figure 3. Simulated XRPD patterns of **1a**−**1e** showing they are not similar yet they are isotypical.

the XRPD patterns of the solvated bulk sample do not match with those of the simulated patterns, it does not mean that they are not isotypical.

Compound **2** has been synthesized as light yellow block crystals by the solvothermal reaction from $Cd(NO_3)_2$ and DPNI in DMA, water and methanol mixture at 90 °C for 48 h. The structure of this compound was determined by single crystal X-ray diffraction experiments, and the PXRD patterns confirmed the phase purity of the bulk. This compound crystallized in monoclinic $P2_1/n$ space group and the asymmetric unit consists of one Cd(II) metal ion, one PNMI, 0.5 DMA and five highly disordered water molecules. In this compound Cd(II) is present in octahedral coordination geometry. Each Cd(II) is coordinated by five carboxylate O atoms from four different PNMI ligands and the coordination geometry is completed by a pyridyl-*N* from another PNMI ligand as shown in Figure 4a. Further, each PNMI is coordinated to four different Cd(II) atoms through carboxylate ligands. One of the carboxylate oxygen atoms, namely, O3 from two different PNMI ligands is bridging axially to one Cd(II) atom and equatorially to another Cd(II) atom forming a four-membered Cd_2O_2 ring and the other three carboxylate O atoms are bonded in a monodentate manner. This connectivity produces a one-dimensional structure aligned along *a*-axis and all these 1-D strips are well-aligned in a herringbone style in the *bc*-plane. The 1-D polymeric strips are interlinked to the four adjacent 1-D strips via Cd−N bonds to create a 3-D structure with 1-D channels all aligned along *a*-axis as shown in Figure 4b.

If one considers the Cd_2O_2 ring as a 6-connected node, then **2** is a network of the same **rtl** net topology as **1** discussed above. In the rhomboidal 1-D channels the diagonal distances from the centers of the Cd_2O_2 ring forming the rhombus structure correspond to the *b*- and *c*-axes of the unit cell 24.836(3) and 20.663(2) Å. However, it may be noted from Figure 4b that they are bent. But the strain at the Cd−pyridine bond has been relieved as compared to **1**. The potential void volume of 1138.8 $Å^3$ (44.9% of the unit cell volume, 2539 $Å^3$) as calculated by the PLATON program, is available for guest molecules upon removal of solvent.[16]

The isomorphous and isostructural Mn(II) compound, **3**·075DMF has been synthesized from $Mn(ClO_4)_2$ in DMF/water solution with DPNI at 80 °C for 60 h. However, in the case of any of these compounds, we observed the exchange of DMA with water and methanol which has been confirmed by TGA. But further exchange with other solvents is not successful from the point of retention of single crystals. This could be explained because of the rigid metal carboxylate aggregates and higher coordination environment in **2** and **3**. On the other hand, the soft SBU[5,6] in the case of **1** appears to favor the exchange of lattice solvents with other guest molecules. The TGA showed that all these compounds **1**−**3** are stable up to 370 to 400 °C (see Supporting Information Figures S5−8).

Gas Sorption Studies. The presence of large channels and good thermal stability of these compounds prompted us to study the gas sorption properties of these compounds. For this purpose, all these compounds has been activated and studied N_2 and H_2 sorption at 1 bar and 77 K. Surprisingly, all these compounds show little or no uptake of N_2 and H_2 gases (see Supporting Information Figure S9). This is probably due to the contraction of the pores under activation conditions and there were little or no accessible pore surface for these gases, which also supported by the shift in the PXRD (0 1 1) peak to higher angles during evacuation of the sample (Supporting Information Figure S4).

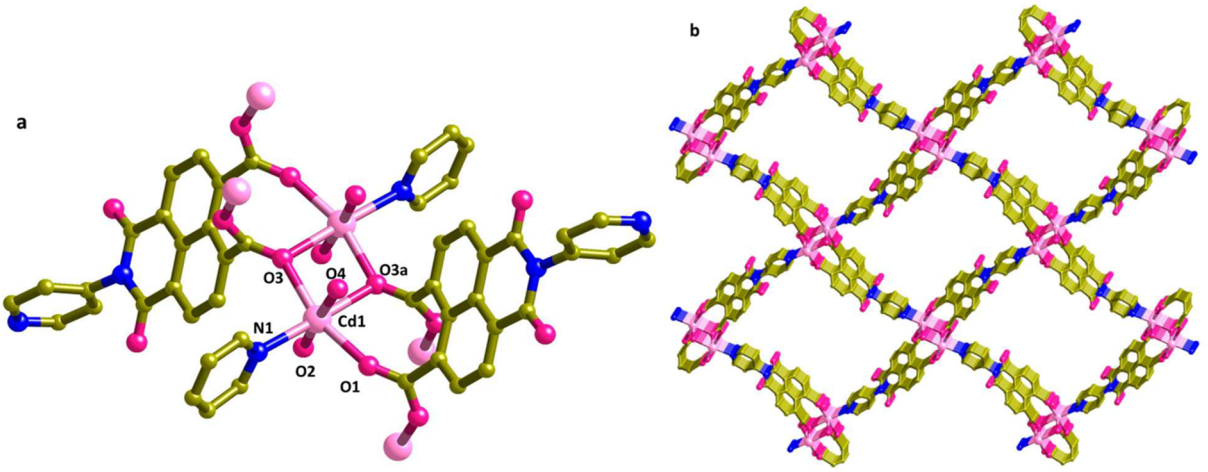

Figure 4. (a) View showing the connectivity and coordination sphere around Cd(II) in **2**. The symmetry operator for O3a is $-x + 1, -y, -z + 1$. (b) Rhombic channel formed by the connectivity in **2** viewed along *a*-axis.

dx.doi.org/10.1021/ic302334x | *Inorg. Chem.* 2013, 52, 2951−2957

On the other hand, the activated **1** and **3** show a small uptake of CO_2 gas (30 and 28 $cm^3 \cdot g^{-1}$, respectively) at 196 K and 1 bar. This small uptake might be due to the approximate match of the increased aperture dimension of accessible pores in these solids with the kinetic diameter (KD) of CO_2 (3.30 Å)[20] at the elevated temperature, 196 K, or the opening of the apertures of some parts of the pores by the highly quadrupole nature CO_2 gas. Activated **2** exhibited better accessibility of the apertures of the most pores and showed significantly increased CO_2 uptake, 278 $cm^3 \cdot g^{-1}$, at 196 K as shown in Figure 5, which corresponds to 5.87 molecules of CO_2 per formula unit of **2.**

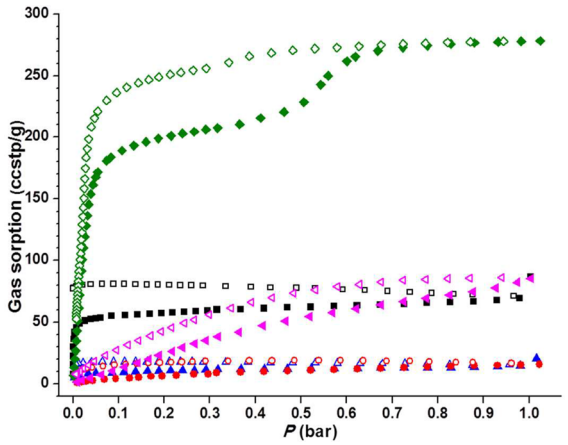

Figure 5. Sorption studies of compound **2**. Green diamond: CO_2 at 196 K. Black squares: N_2 at 77 K. Magenta inverted triangles: CH_4 at 196 K. Red circles: H_2 at 77 K. Blue triangles: Ar at 87 K.

It is noted that in the adsorption plot of CO_2 gas consists of stepwise-rise CO_2 uptake at 0.5 bar with hysteresis. However, the stepwise adsorption usually observed either by a compound which consist of different sized pores or with the pore with different interactions/functional groups exposed at the pores. In case of **2**, all 1D pores are of the same size with uniform functional groups on the walls. Therefore, the step in CO_2 adsorption plot might be attributed to the dynamic nature of the framework.[21] The hysteresis might have been caused by the strong interaction of the adsorbate CO_2 gas with the polar framework and the interaction resulted in some structural change of the framework at ~0.5 bar. Such "breathing behavior" in response to adsorbed guest molecules has been observed in many soft porous networks.[3f,h,5,17c] This is again due to large quadrupole moment (13.4 $C \cdot m^2$) and polarizability (2.93)[20] of CO_2, which enable CO_2 to interact with the highly polar imide oxygen atoms in the channels and showed better adsorption compared to other gases with isosteric heat of adsorption of ~24 KJ/mol at initial stages of adsorption and slightly reduced at the initial stages of adsorption and increased again, this also support the dynamic nature of framework (Supporting Information Figure S11). As there is little adsorption of N_2 gas, surface area of **2** has been estimated by using CO_2 adsorption at 196 K, which shows the BET and Langmuir surface areas as 1130 and 1670 $m^2 \cdot g^{-1}$ respectively. Similarly, the sorption study of few other samples, such as H_2 at 77 K, Ar at 87 K, and CH_4 at 196 K has been studied (Figure 5). As expected, the polar imide pores selectively adsorbing highly quadrupolar CO_2 from other gases at 196 K. Such selective adsorption for CO_2 over other gases is advantageous for the separation of gas mixtures. Very recently, an MOF with a similar 1D hexagonal pore was found to show similar sorption properties has been reported.[21b]

CONCLUSION

During the solvothermal synthesis, DPNI was partially hydrolyzed to PNMI and provided two structurally similar yet distinct MOF structures showing large rhomboidal channels all aligned in parallel. The structure of **1** is built from paddle-wheel SBU, while isotypical **2** and **3** are made up of one-dimensional aggregates of $M(O_2C{-}C)_2$ in the framework. The guest molecules in **1a** can be exchanged with EtOH in an SCSC manner to **1b** which in turn has been successfully used to reversibly exchange with EG and TEGly and allyl alcohol without destroying its single crystal nature. Among all these three guest molecules, the EtOH in **1**b can be selectively exchanged with TEGly which may be attributed to correct fit of the hydrogen-bonded TEGly dimer in the pores of **1**. These SCSC exchanges are accompanied by reduction of the volume of the unit cell up to 16% and the void volume up to 33.1%. The decrease in the void volume suggests that the soft and flexible nature of the structure and the retention of the structure upon removal of the solvents were shown by the PXRD experiments. To investigate this behavior, sorption studies were undertaken and found that all these activated MOFs exhibits very low or no uptake of H_2 and N_2 gases at 1 bar and 77 K, but better adsorption of CO_2 with hysteresis. On the other hand, the activated **2** shows selective CO_2 uptake over H_2, N_2, Ar, and CH_4 and hence would be promising for separation of gas mixtures.

ASSOCIATED CONTENT

Supporting Information

Some more metric information, crystallographic information, PXRD and TGA curves. This material is available free of charge via the Internet at http://pubs.acs.org. The CIF files can be obtained free of charge from the Cambridge Crystallographic Data Centre via www.ccdc.cam.ac.uk/data_request/cif CCDC Numbers 893751−893757 (for compounds **1**−**3**) for this paper.

AUTHOR INFORMATION

Corresponding Author

*Fax: (+82) 55-753-7614 (S.S.L.); (+82) 52-217-2019 (M.S.L.); (+65) 67791691 (J.J.V.). E-mail: sslee@gnu.ac.kr (S.S.L.); mslah@unist.ac.kr (M.S.L.); chmjjv@nus.edu.sg (J.J.V.).

Notes

The authors declare no competing financial interest.

ACKNOWLEDGMENTS

J.J.V. would like to thank the Ministry of Education, Singapore for financial support (through NUS FRC Grant R-143-000-439-112) and the Ministry of Education, Science & Technology, S. Korea for the WCU Chair Professorship. J.J.V. and S.S.L. acknowledges the funding from the World Class University (WCU) project (R32-20003). M.S.L. thanks the National Research Foundation of Korea for financial support (NRF-2011-0027950).

REFERENCES

(1) (a) Stock, N.; Biswas, S. *Chem. Rev.* **2011**, *112*, 933. (b) Schoedel, A.; Wojtas, L.; Kelley, S. P.; Rogers, R. D.; Eddaoudi, M.; Zaworotko,

M. J. *Angew. Chem., Int. Ed.* **2011**, *50*, 11421. (c) Hill, R. J.; Long, D.-L.; Champness, N. R.; Hubberstey, P.; Schröder, M. *Acc. Chem. Res.* **2005**, *38*, 335.
(2) (a) Suh, M. P.; Park, H. J.; Prasad, T. K.; Lim, D.-W. *Chem. Rev.* **2011**, *112*, 782. (b) Li, J.-R.; Kuppler, R. J.; Zhou, H.-C. *Chem. Soc. Rev.* **2009**, *38*, 1477. (c) Sumida, K.; Rogow, D. L.; Mason, J. A.; McDonald, T. M.; Bloch, E. D.; Herm, Z. R.; Bae, T.-H.; Long, J. R. *Chem. Rev.* **2011**, *112*, 724. (d) Li, J.-R.; Sculley, J.; Zhou, H.-C. *Chem. Rev.* **2011**, *112*, 869. (e) Yoon, M.; Srirambalaji, R.; Kim, K. *Chem. Rev.* **2011**, *112*, 1196. (f) Nagarathinam, M.; Saravanan, K.; Phua, E. J. H.; Reddy, M. V.; Chowdari, B. V. R.; Vittal, J. J. *Angew. Chem., Int. Ed.* **2012**, *51*, 5866. (g) Kreno, L. E.; Leong, K.; Farha, O. K.; Allendorf, M.; Van Duyne, R. P.; Hupp, J. T. *Chem. Rev.* **2012**, *112*, 1196.
(3) (a) Choi, H.-S.; Suh, M. P. *Angew. Chem., Int. Ed.* **2009**, *48*, 6865. (b) Demessence, A.; Long, J. R. *Chem.—Eur. J.* **2010**, *16*, 5902. (c) Wu, H.; Reali, R. S.; Smith, D. A.; Trachtenberg, M. C.; Li, J. *Chem.—Eur. J.* **2010**, *16*, 13951. (d) Higuchi, M.; Nakamura, K.; Horike, S.; Hijikata, Y.; Yanai, N.; Fukushima, T.; Kim, J.; Kato, K.; Takata, M.; Watanabe, D.; Oshima, S.; Kitagawa, S. *Angew. Chem., Int. Ed.* **2012**, *51*, 8369. (e) Horcajada, P.; Serre, C.; Maurin, G.; Ramsahye, N. A.; Balas, F.; Vallet-Regí, M. a.; Sebban, M.; Taulelle, F.; Férey, G. *J. Am. Chem. Soc.* **2008**, *130*, 6774. (f) Férey, G.; Serre, C. *Chem. Soc. Rev.* **2009**, *38*, 1380. (g) Kitagawa, S.; Kitaura, R.; Noro, S.-I. *Angew. Chem., Int. Ed.* **2004**, *43*, 2334. (h) Kitaura, R.; Seki, K.; Akiyama, G.; Kitagawa, S. *Angew. Chem., Int. Ed.* **2003**, *42*, 428.
(4) (a) Kim, T. K.; Suh, M. P. *Chem. Commun.* **2011**, *47*, 4258. (b) Thallapally, P. K.; Tian, J.; Radha Kishan, M.; Fernandez, C. A.; Dalgarno, S. J.; McGrail, P. B.; Warren, J. E.; Atwood, J. L. *J. Am. Chem. Soc.* **2008**, *130*, 16842. (c) Xie, L.-H.; Suh, M. P. *Chem.—Eur. J.* **2011**, *17*, 13653.
(5) Seo, J.; Bonneau, C.; Matsuda, R.; Takata, M.; Kitagawa, S. *J. Am. Chem. Soc.* **2011**, *133*, 9005.
(6) Bureekaew, S.; Amirjalayer, S.; Schmid, R. *J. Mater. Chem* **2012**, *22*, 10249.
(7) (a) Wu, C.-D.; Lin, W. *Angew. Chem., Int. Ed.* **2005**, *44*, 1958. (b) Das, M. C.; Bharadwaj, P. K. *J. Am. Chem. Soc.* **2009**, *131*, 10942. (c) Sharma, M. K.; Lama, P.; Bharadwaj, P. K. *Cryst. Growth. Des.* **2011**, *11*, 1411.
(8) Allan, P. K.; Xiao, B.; Teat, S. J.; Knight, J. W.; Morris, R. E. *J. Am. Chem. Soc.* **2010**, *132*, 3605.
(9) Yang, S.; Lin, X.; Lewis, W.; Suyetin, M.; Bichoutskaia, E.; Parker, J. E.; Tang, C. C.; Allan, D. R.; Rizkallah, P. J.; Hubberstey, P.; Champness, N. R.; Mark Thomas, K.; Blake, A. J.; Schröder, M. *Nat. Mater.* **2012**, *11*, 710.
(10) (a) Mulfort, K. L.; Farha, O. K.; Malliakas, C. D.; Kanatzidis, M. G.; Hupp, J. T. *Chem.—Eur. J.* **2010**, *16*, 276. (b) Vaidhyanathan, R.; Iremonger, S. S.; Shimizu, G. K. H.; Boyd, P. G.; Alavi, S.; Woo, T. K. *Science* **2010**, *330*, 650. (c) Kanoo, P.; Ghosh, A. C.; Cyriac, S. T.; Maji, T. K. *Chem.—Eur. J.* **2012**, *18*, 237.
(11) Farha, O. K.; Malliakas, C. D.; Kanatzidis, M. G.; Hupp, J. T. *J. Am. Chem. Soc.* **2010**, *132*, 950.
(12) Sheldrick, G. M. *SADABS*; University of Göttingen: Göttingen, Germany, 1996.
(13) (a) Sheldrick, G. M. *Acta Crystallogr., Sect. A.* **2008**, *64*, 112. (b) Müller, P.; Herbst-Irmer, R.; L.Spek, A.; R.Schneider, T.; R.Sawaya, M. *Crystal Structure Refinement: A Crystallographer's Guide to SHELXL*; Oxford University Press: Oxford, U.K., 2006.
(14) (a) Ma, B.-Q.; Mulfort, K. L.; Hupp, J. T. *Inorg. Chem.* **2005**, *44*, 4912. (b) Furukawa, S.; Hirai, K.; Takashima, Y.; Nakagawa, K.; Kondo, M.; Tsuruoka, T.; Sakata, O.; Kitagawa, S. *Chem. Commun.* **2009**, 5097. (c) Nelson, A. P.; Parrish, D. A.; Cambrea, L. R.; Baldwin, L. C.; Trivedi, N. J.; Mulfort, K. L.; Farha, O. K.; Hupp, J. T. *Cryst. Growth. Des.* **2009**, *9*, 4588. (d) Chung, H.; Barron, P. M.; Novotny, R. W.; Son, H.-T.; Hu, C.; Choe, W. *Cryst. Growth. Des.* **2009**, *9*, 3327. (e) Takashima, Y.; Martínez, V. M.; Furukawa, S.; Kondo, M.; Shimomura, S.; Uehara, H.; Nakahama, M.; Sugimoto, K.; Kitagawa, S. *Nat Commun* **2011**, *2*, 168. (f) Burnett, B. J.; Barron, P. M.; Hu, C.; Choe, W. *J. Am. Chem. Soc.* **2011**, *133*, 9984.
(15) (a) Blatov, V. A. *TOPOS, A Multipurpose Crystallochemical Analysis with the Program Package*; Samara State University: Samara, Russia, 2009. (b) Blatov, V. A. *IUCr Comp. Commun. News. Lett.* **2006**, *7*, 4. (c) Alexandrov, E. V.; Blatov, V. A.; Kochetkov, A. V.; Proserpio, D. M. *Cryst. Eng. Commun.* **2011**, *13*, 3947.
(16) Spek, A. L. *J. Appl. Crystallogr.* **2003**, *36*, 7.
(17) (a) Férey, G.; Mellot-Draznieks, C.; Serre, C.; Millange, F.; Dutour, J.; Surblé, S.; Margiolaki, I. *Science* **2005**, *309*, 2040. (b) Lu, J. Y.; Babb, A. M. *Chem. Commun.* **2002**, 1340. (c) Henke, S.; Schneemann, A.; Wütscher, A.; Fischer, R. A. *J. Am. Chem. Soc.* **2012**, *134*, 9464. (d) Ferey, G.; Latroche, M.; Serre, C.; Millange, F.; Loiseau, T.; Percheron-Guegan, A. *Chem. Commun.* **2003**, 2976.
(18) Pirondini, L.; Stendardo, A. G.; Geremia, S.; Campagnolo, M.; Samorì, P.; Rabe, J. P.; Fokkens, R.; Dalcanale, E. *Angew. Chem., Int. Ed.* **2003**, *42*, 1384.
(19) (a) Chen, B.; Liang, C.; Yang, J.; Contreras, D. S.; Clancy, Y. L.; Lobkovsky, E. B.; Yaghi, O. M.; Dai, S. *Angew. Chem., Int. Ed.* **2006**, *45*, 1390. (b) Choi, H. J.; Dincă, M.; Long, J. R. *J. Am. Chem. Soc.* **2008**, *130*, 7848.
(20) Breck, D. W., *Zeolite Molecular Sieves*; Wiley & Sons: New York, 1974.
(21) (a) Yuan, D.; Getman, R. B.; Wei, Z.; Snurr, R. Q.; Zhou, H.-C. *Chem. Commun.* **2012**, *48*, 3297. (b) Hawes, C. S.; Babarao, R.; Hill, M. R.; White, K. F.; Abrahams, B. F.; Kruger, P. E. *Chem. Commun.* **2012**, *48*, 11558. (c) Salles, F.; Maurin, G.; Serre, C.; Llewellyn, P. L.; Knöfel, C.; Choi, H. J.; Filinchuk, Y.; Oliviero, L.; Vimont, A.; Long, J. R.; Férey, G. r. *J. Am. Chem. Soc.* **2010**, *132*, 13782. (d) Kondo, A.; Noguchi, H.; Carlucci, L.; Proserpio, D. M.; Ciani, G.; Kajiro, H.; Ohba, T.; Kanoh, H.; Kaneko, K. *J. Am. Chem. Soc.* **2007**, *129*, 12362.